



ELSEVIER

Journal of Chromatography A, 680 (1994) 599–607

JOURNAL OF
CHROMATOGRAPHY A

Capillary electrophoretic chiral separations using cyclodextrin additives

III. Peak resolution surfaces for ibuprofen and homatropine as a function of the pH and the concentration of β -cyclodextrin

Yasir Y. Rawjee¹, Robert L. Williams, Gyula Vigh*

Chemistry Department, Texas A & M University, College Station, TX 77843-3255, USA

Abstract

Our recent extended peak resolution equation of capillary electrophoresis has been combined with the multiple equilibria-based electrophoretic mobility model of chiral separations to describe peak resolution as a function of the composition of the background electrolyte (pH and the β -cyclodextrin concentration) and a function of the operating variables (effective portion of the applied potential, dimensionless electroosmotic flow coefficient). Using the previously determined model parameters, the resolution surfaces were calculated for a Type I chiral separation (ibuprofen), and a Type III chiral separation (homatropine). In Type I separations resolution can be obtained only over a narrow pH range in the vicinity of the pK_a value, and above a minimum value, the concentration of β -cyclodextrin plays a lesser role. In Type III separations, the pH- and β -cyclodextrin concentration-dependent resolution surface has two lobes, on which the migration order of the enantiomers is opposite. This can be an advantage in trace component analysis. In both Type I and Type III separations, peak resolution varies strongly with the dimensionless electroosmotic flow coefficient when its value is changed in the -1 to 1 range. The loci of the pH-dependent and the β -cyclodextrin concentration-dependent resolution maxima do not shift significantly when the dimensionless electroosmotic flow coefficient is changed. This fact provides the analyst with an additional resolution enhancement tool that does not alter the selectivity of the separation. The utility of the model and its theoretical predictions has been demonstrated by comparing measured and calculated R_s values for ibuprofen and homatropine.

1. Introduction

In Parts I and II of this series of papers, which deal with the separation of enantiomers by capillary electrophoresis (CE), we introduced an equilibrium model that describes separation

selectivity as a function of the pH and the β -cyclodextrin (CD) concentration of the background electrolyte (BGE) [1,2]. Using the electroosmotic flow-corrected effective mobilities of the enantiomers, measured in three specifically designed sets of BGEs, we were able to determine the model parameters: the acid dissociation constant, the apparent complex formation constants between CD and the dissociated enantiomers, the apparent complex formation con-

* Corresponding author.

¹ Present address: Smith-Kline Beecham, King of Prussia, PA 19406, USA.

stants between CD and the non-dissociated enantiomers, the ionic mobilities of the dissociated non-complexed enantiomers and the ionic mobilities of the dissociated complexed enantiomers. The model indicated the existence of three fundamentally different types of enantiomer separations depending on whether (i) only the non-ionic forms of the two enantiomers, (ii) only the ionic forms of the two enantiomers, or (iii) both forms of the two enantiomers interact differently with CD.

Subsequently, we modified the general peak resolution equation to express peak resolution as a function of the separation selectivity, the effective charge of the enantiomers, and the dimensionless electroosmotic flow [3,4]. This resolution expression incorporates, as a limiting case, the equation proposed by Friedl and Kenndler [5], which is applicable in the absence of electroosmotic flow. In this paper, we combine the extended peak resolution equation [3,4] with the selectivity data we obtained for weak acid [1] and weak base enantiomers [2] using native β -cyclodextrin as resolving agent. We will compare the emerging optimization schemes with the recommendations made in Parts I and II that were based solely on separation selectivity data.

2. Theory

According to Refs. [3] and [4], peak resolution in chiral CE can be described as:

$$R_s = \sqrt{\frac{E l e_0}{8 k T}} \cdot \frac{|\alpha - 1| \sqrt{|\alpha + \beta|} \sqrt{|1 + \beta|} \sqrt{z_R^{\text{eff}}} \sqrt{z_S^{\text{eff}}}}{\sqrt{(\alpha + \beta)^3 |z_R^{\text{eff}}| + \sqrt{\alpha} (1 + \beta)^3 |z_S^{\text{eff}}|}} \quad (1)$$

where E is the field strength, l the length of the capillary from injector to detector, e_0 the electric charge, k the Boltzman constant, T the absolute temperature, α the separation selectivity, β the dimensionless coefficient of the electroosmotic flow, z_R^{eff} the effective charge of the R enantiomer and z_S^{eff} the effective charge of the S

enantiomer. In turn, separation selectivity is defined as:

$$\alpha = \frac{\mu_R^{\text{eff}}}{\mu_S^{\text{eff}}} \quad (2)$$

with

$$\mu_R^{\text{obs}} = \mu_R^{\text{eff}} + \mu_{\text{eo}} \quad (3)$$

where μ_R^{obs} is the observed mobility of the R enantiomer, μ_R^{eff} is the effective mobility of the R enantiomer, and μ_{eo} is the coefficient of the electroosmotic flow. The dimensionless coefficient of the electroosmotic flow, β , is defined as:

$$\beta = \frac{\mu_{\text{eo}}}{\mu_S^{\text{eff}}} \quad (4)$$

Eq. 1 is applicable for the $-\infty < \beta \leq -\alpha$ and $-1 \leq \beta < \infty$ ranges. This is so, because according to its classical definition, R_s has no meaning in the $-\alpha \leq \beta \leq -1$ range, where only one of the enantiomers can migrate past the detector (the more mobile enantiomer in the $-\alpha < \beta \leq -1$ range, and the less mobile enantiomer in the $\beta = -\alpha$ point).

In a BGE which contains CD as the chiral resolving agent and the enantiomers of a weak acid analyte, HR and HS, acid dissociation ($\text{HR} + \text{H}_2\text{O} \rightleftharpoons \text{R}^- + \text{H}_3\text{O}^+$) and complex formation ($\text{HR} + \text{CD} \rightleftharpoons \text{HRCD}$ and $\text{R}^- + \text{CD} \rightleftharpoons \text{RCD}^-$) reactions will occur. (Only the reactions of the R enantiomer are shown.) The apparent equilibrium constants for these reactions are K_{HR} , K_{HRCD} and K_{RCD^-} . The effective mobility of the R enantiomer, μ_R^{eff} , is a linear combination of the mole fractions and the ionic mobilities of the respective species [1]:

$$\mu_R^{\text{eff}} = \frac{\mu_{\text{R}^-}^0 + \mu_{\text{RCD}^-}^0 - K_{\text{RCD}^-} [\text{CD}]}{1 + K_{\text{RCD}^-} [\text{CD}] + \frac{[\text{H}_3\text{O}^+]}{K_{\text{HR}}} \cdot (1 + K_{\text{HRCD}} [\text{CD}])} \quad (5)$$

where $\mu_{\text{R}^-}^0$ and $\mu_{\text{RCD}^-}^0$ are the ionic mobilities of the non-complexed and complexed, fully dissociated enantiomers, respectively.

The effective charge of the R enantiomer, z_R^{eff} ,

is a linear combination of the mole fractions and the ionic charges of the respective species [3,4]:

$$z_R^{\text{eff}} = \frac{z_{R^-}^0 + z_{RCD^-}^0 - K_{RCD^-}[\text{CD}]}{1 + K_{RCD^-}[\text{CD}] + \frac{[\text{H}_3\text{O}^+]}{K_{\text{HR}}} \cdot (1 + K_{\text{HRCD}}[\text{CD}])} \quad (6)$$

where $z_{R^-}^0$ and $z_{RCD^-}^0$ are the ionic charges of the non-complexed fully dissociated enantiomers, and the complexed fully dissociated enantiomers, respectively. Similar expressions exist for the *S* enantiomer. With these expressions, separation selectivity, α , becomes:

$$\alpha = \frac{\mu_{R^-}^0 + \mu_{RCD^-}^0 - K_{RCD^-}[\text{CD}]}{\mu_{S^-}^0 + \mu_{SCD^-}^0 - K_{SCD^-}[\text{CD}]} \cdot \frac{1 + K_{SCD^-}[\text{CD}] + \frac{[\text{H}_3\text{O}^+]}{K_a} \cdot (1 + K_{\text{HS}}[\text{CD}])}{1 + K_{RCD^-}[\text{CD}] + \frac{[\text{H}_3\text{O}^+]}{K_a} \cdot (1 + K_{\text{HRCD}}[\text{CD}])} \quad (7)$$

since the non-complexed enantiomers have identical ionic mobilities and acid dissociation constants ($\mu_{R^-}^0 = \mu_{S^-}^0 = \mu_-^0$ and $K_{\text{HR}} = K_{\text{HS}} = K_a$).

Eqs. 1 and 4–7 predict that peak resolution depends on operator-dependent parameters (effective portion of the applied potential, temperature, concentration of CD, pH, coefficient of the electroosmotic flow) and solute specific parameters (acid dissociation constant, ionic charges and ionic mobilities for the non-complexed and the complexed enantiomers, complex formation constants for the dissociated enantiomers and the non-dissociated enantiomers). Analogous expressions (in terms of $[\text{OH}^-]$) can be derived for weak base analytes [2,4].

Since the ionic charges of the *R* and *S* enantiomers are identical in both the CD-complexed and non-complexed forms ($z_{R^-}^0 = z_{S^-}^0$ and $z_{RCD^-}^0 = z_{SCD^-}^0$), the solute specific parameters that determine the shape of the peak resolution surface and the separation selectivity surface are the same. Therefore, it can be expected that

there will be three different types of resolution surfaces (as there are three different types of selectivity surfaces), depending on whether (i) only the non-ionic forms of the two enantiomers, (ii) only the ionic forms of the two enantiomers, or (iii) both forms of the two enantiomers interact differently with CD. In *Type I* separations, $K_{\text{HRCD}} \neq K_{\text{HS}}[\text{CD}]$, $K_{RCD^-} = K_{SCD^-}$ and $\mu_{RCD^-}^0 = \mu_{SCD^-}^0$, which reduces the first term of Eq. 7 to unity. In *Type II* separations, $K_{\text{HRCD}} = K_{\text{HS}}[\text{CD}]$, $K_{RCD^-} \neq K_{SCD^-}$ and $\mu_{RCD^-}^0 \neq \mu_{SCD^-}^0$, which means that the first and second terms of Eq. 7 have opposing effects on the separation and can result in $\alpha < 1$, $\alpha = 1$ and $\alpha > 1$ with an accompanying reversal of the migration order. In *Type III* separations, $K_{\text{HRCD}} \neq K_{\text{HS}}[\text{CD}]$, $K_{RCD^-} \neq K_{SCD^-}$ and $\mu_{RCD^-}^0 \neq \mu_{SCD^-}^0$, which again means that the first and second terms of Eq. 7 have opposing effects on the separation and can result in $\alpha < 1$, $\alpha = 1$ and $\alpha > 1$ and can provide reversed migration orders. In order to test these possibilities, the resolution surfaces for ibuprofen and homatropine, a chiral weak acid and a chiral weak base, have been calculated using the data published in Refs. [1] and [2].

3. Experimental

The experimental conditions were described in detail in Refs. [1] and [2]; all data used in the present paper are taken from these measurements [except in Fig. 7, where LiOH was replaced with Jeffamine 900 (Sigma, St. Louis, MO, USA) as base]. All calculations have been carried out on a 486DX33 personal computer (Computer Access, College Station, TX, USA) using the Origin Version 3.0 software package (MicroCal Software, Northampton, MA, USA).

4. Results and discussion

Table 1 lists the model parameters for ibuprofen [1] and homatropine [2]. These parameters, coupled with $E = 600$ V/cm, $l = 39.5$ cm

Table 1
Ionic mobility and apparent equilibrium constant data for ibuprofen [1] and homatropine [2] at 37°C

Ibuprofen		Homatropine	
Parameter	Value	Parameter	Value
K_a	$3.3 \cdot 10^{-5}$	K_a	$2.9 \cdot 10^{-10}$
μ_-^0 (cm ² /V s)	$21.3 \cdot 10^{-5}$	μ_+^0 (cm ² /V s)	$23.4 \cdot 10^{-5}$
$\mu_{RCD^-}^0$ (cm ² /V s)	$6.6 \cdot 10^{-5}$	$\mu_{HRCD^0}^0$ (cm ² /V s)	$9.2 \cdot 10^{-5}$
$\mu_{SCD^-}^0$ (cm ² /V s)	$6.6 \cdot 10^{-5}$	$\mu_{HSCD^+}^0$ (cm ² /V s)	$9.2 \cdot 10^{-5}$
K_{RCD^-}	1280	K_{HRCD^+}	88
K_{SCD^-}	1280	K_{HSCD^+}	104
K_{HRCD}	1869	K_{RCD}	1305
K_{HSCD}	1954	K_{SCD}	1350

and $T = 37^\circ\text{C}$ were used here for the calculation of the peak resolution surfaces.

The three-dimensional peak resolution surface and its contour map for ibuprofen, a Type I separation, are shown in Fig. 1. The surface was calculated for $\beta = 0$ (no electroosmotic flow), and no electromigration dispersion. Along the pH axis, the resolution surface is dominated by a very-well-defined ridge in the vicinity of the pK_a value. It is very important to note that this ridge spans only about 2 pH units at $R_s = 1$, meaning that in the case of a Type I separation it is very

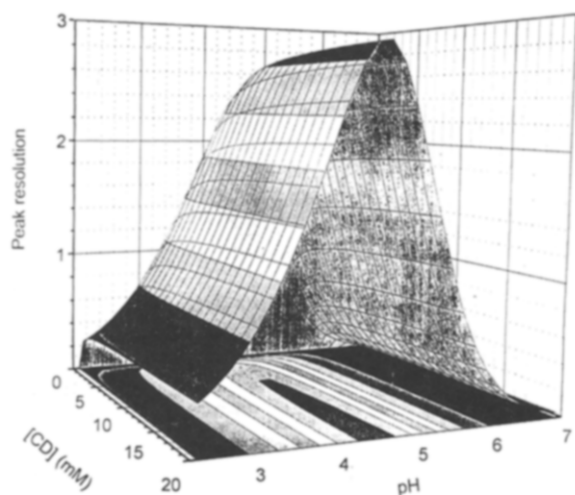


Fig. 1. Peak resolution surface for the enantiomers of ibuprofen as a function of the pH and the β -cyclodextrin concentration of the background electrolyte, calculated with $\beta = 0$, $E = 600$ V/cm, $l = 39.5$ cm, $T = 310$ K and the parameters listed in Table 1.

easy to miss the pH range where enantiomer separation can be achieved at all. Across the cyclodextrin concentration axis, R_s first increases very rapidly, then, above 10 mM CD, it begins to level off towards a limiting high value. This means that from an optimization point of view the exact concentration of β -cyclodextrin is not too important, it only has to exceed a minimum value.

The prominent pH-dependent R_s maximum can be rationalized by considering that at high pH there is no resolution at any CD concentration because α is unity due to $K_{RCD^-} = K_{SCD^-}$. As the pH is decreased, the mole fractions of the non-dissociated enantiomers become larger resulting in increased α (cf. Fig. 16 in Ref. [1]). As pH is further decreased to a value which is below the pK_a value, the effective charge of the enantiomers (z^{eff}) decreases rapidly (cf. Eq. 6) which, according to Eq. 1, lowers the value of R_s and results in an R_s maximum.

The peak resolution surface shown in Fig. 1 confirms the operating condition selections recommended in Ref. [1], which were based on the selectivity surface: "In the case of a Type I enantiomer (separation) . . . optimization of the separation (is) simple: the pH of the background electrolyte must be decreased until the selectivity becomes sufficiently high so that the desired peak resolution is realized with the available separation efficiency resulting, automatically, in the shortest possible separation time".

Since Fig. 1 has been calculated for $\beta = 0$, it is

instructive to see what happens to peak resolution in the presence of electroosmotic flow. According to Fig. 1, at high CD concentrations R_s is almost invariant in [CD]. Therefore, a constant CD concentration that is close to the solubility limit was selected, [CD] = 15 mM, and pH was varied between 2 and 6, while β was varied between -3 and 3 . The calculated resolution surface is shown in Fig. 2. The pH effects are similar to those that were observed in Fig. 1. As expected from Eq. 1, R_s improves very rapidly as the condition $\beta = -1$ is approached in the $-1 < \beta < \infty$ range, and as the condition $\beta = -\alpha$ is approached in the $-\infty < \beta < -\alpha$ range. If one uses an uncoated fused-silica capillary, the direction of the electroosmotic flow is opposite to that of the electrophoretic migration of the negatively charged ibuprofen enantiomers. The magnitude of the electroosmotic flow can be reduced easily by adding hydroxyethylcellulose to the BGE. As the electroosmotic flow is gradually suppressed, improvement in R_s is comparatively small in the $-10 < \beta < -3$ range. However, as β enters the $-2 < \beta < -1$ range, R_s improves tremendously. If the electroosmotic flow is depressed even further, and one crosses over into the $-1 < \beta < 0$ range, the absolute

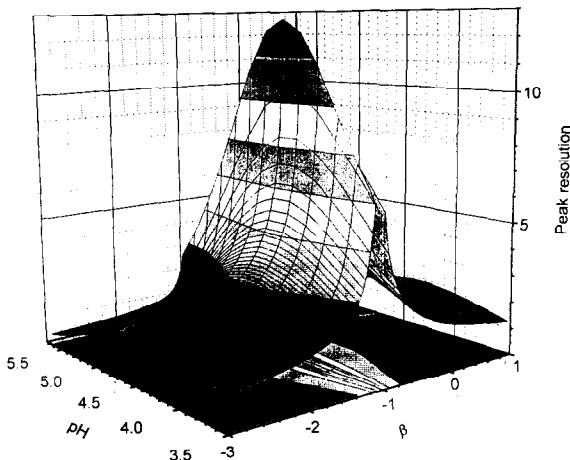


Fig. 2. Peak resolution surface for the enantiomers of ibuprofen as a function of the pH of the background electrolyte and the dimensionless electroosmotic flow coefficient, β , calculated with $E = 600$ V/cm, $l = 39.5$ cm, $T = 310$ K, [CD] = 15 mM and the parameters listed in Table 1.

value of the electrophoretic mobility of ibuprofen becomes larger than that of the electroosmotic flow, meaning that ibuprofen is carried through the capillary electrophoretically, rather than electroosmotically as in the $-10 < \beta < -1$ range. R_s is high as long as $-1 < \beta < -0.5$. In a pH 4.5 background electrolyte (close to the crest of the resolution surface), it is very easy to create such conditions by adding just enough hydroxyethylcellulose to sufficiently (but not excessively) depress the naturally weak electroosmotic flow, as demonstrated by the successful separation of the ibuprofen enantiomers in Fig. 17 in Ref. [1]. It is more difficult to probe the $0 < \beta$ range, because one has to use a capillary that has positive surface charges.

One can compare the peak resolution values calculated from the model parameters, the applicable field strength and electroosmotic flow velocities with the experimentally determined ones obtained in a series of measurements using [CD] = 15 mM background electrolytes in which the pH was varied between 4.1 and 5.3 (data taken from Fig. 13 in Ref. [1]). As shown in Fig. 3, the calculated and measured resolution values follow the same trend, have their maximum at

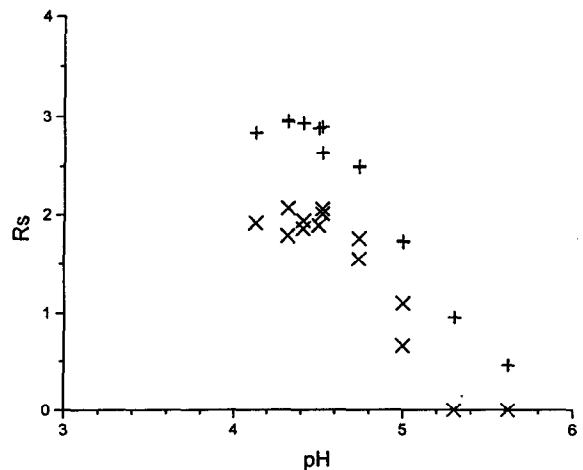


Fig. 3. Comparison of the measured and calculated peak resolution values for the enantiomers of ibuprofen as a function of the pH at a CD concentration of 15 mM, 200 V/cm $< E < 700$ V/cm, $-0.95 < \beta < 0$. Measured data and the conditions are from Fig. 13 in Ref. [1]. \times = Measured values; $+$ = calculated values.

the same pH, indicating that the peak resolution model is suitable for separation optimization. Due to the presence of electromigration dispersion, the measured peak resolution values are about 25 to 30% lower than the predicted ones. The peak resolution surface for homatropine, representing a Type III separation, is shown in Fig. 4. The surface has two lobes, which are separated by an $R_s = 0$ line. The primary lobe is the one at low pH. Peak resolution on the primary (low pH) lobe is high for two reasons. First, the weak base is fully protonated at low pH, therefore α is high, because $K_{\text{HRC}^+} \neq K_{\text{HSC}^+}$ (cf. Eq. 7 and Fig. 8 in Ref. [2]). Second, at low pH, $z_R^{\text{eff}} = 1$ and $z_S^{\text{eff}} = 1$, which increases the value of R_s according to Eq. 1. On the primary lobe, R_s passes a maximum as the concentration of CD is increased. In the case of homatropine, this maximum would occur at 20 mM, a CD concentration that is slightly higher than the solubility limit of CD.

Part of the secondary lobe is visible in Fig. 4; it is at high pH and at high CD concentrations. One can cross over from the primary lobe to the secondary lobe by keeping the cyclodextrin concentration constant (e.g. at 20 mM) and increasing the pH towards —and beyond— the $\text{p}K_a$

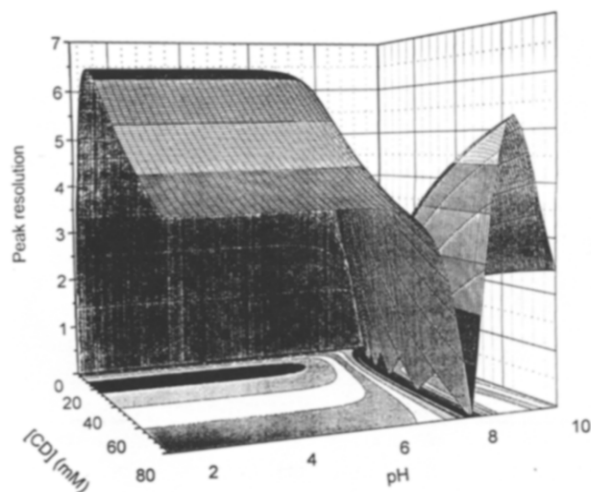


Fig. 4. Peak resolution surface for the enantiomers of homatropine as a function of the pH and the β -cyclodextrin concentration of the background electrolyte, calculated with $\beta = 0$, $E = 600$ V/cm, $l = 39.5$ cm, $T = 310$ K and the parameters listed in Table 1.

value of the conjugate acid. During this process R_s first decreases, becomes zero, then increases again, albeit with a reversed migration order. Reversal of the migration order is caused by the change of α from $\alpha > 1$ to $\alpha < 1$ (cf. Eq. 7 and Fig. 8 in Ref. [2]). Unfortunately, for homatropine, R_s is so small on the experimentally accessible part of the secondary lobe (high pH, low CD concentration) that it is of not much practical significance.

The peak resolution surface shown in Fig. 4 agrees with the recommendations made in Ref. [2]: "... (for) homatropine, ... a Type III ... (separation), one may conclude that the best optimization strategy would call for CD concentrations that are close to the solubility limit (15 mM is safe) and BGE pH values that are at or below pH 7, providing the highest selectivity in the shortest separation time".

Once again it is instructive to see the effects of the electroosmotic flow upon the peak resolution. In Fig. 5, the R_s values were calculated for constant 15 mM CD concentration, while the pH was varied between 5 and 9 (the region where most of the pH-induced R_s change occurs in Fig. 3). β was varied between -3 and 3 . R_s is practically invariant in pH as long as $\text{pH} < 6.5$.

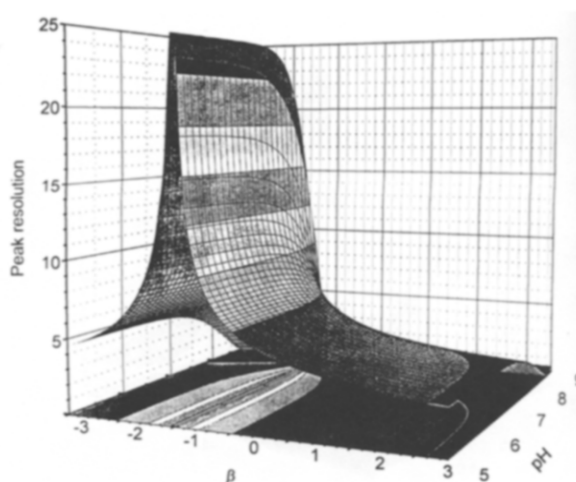


Fig. 5. Peak resolution surface for the enantiomers of homatropine as a function of the pH of the background electrolyte and the dimensionless electroosmotic flow coefficient, β , calculated with $E = 600$ V/cm, $l = 39.5$ cm, $T = 310$ K, $[\text{CD}] = 15$ mM and the parameters listed in Table 1.

The electroosmotic flow has a large effect on R_s when $-1 < \beta < 1$. While experimentally it is somewhat difficult to produce $-1 < \beta < 0$ values (it requires the use of a capillary with a positive charge on its surface), it is relatively easy to obtain $0 < \beta < 1$ values by simply adding hydroxyethylcellulose to the acidic BGEs (pH < 6). In Fig. 6, the R_s values were calculated for constant pH (pH 6.0), varying CD concentrations (0 to 30 mM) and varying β (from -3 to 3). The shallow maximum of R_s , first seen in Fig. 4, is retained while β is changed over a broad range. Again, the electroosmotic flow has a large effect on R_s when $-1 < \beta < 1$, of which the $0 < \beta < 1$ range is easily accessible experimentally as discussed above.

In order to test the applicability of these theoretical predictions, the R_s values were determined from the electropherograms used to construct Fig. 5 in Ref. [2]. The homatropine enantiomer peaks were strongly tailing in these electropherograms due to the presence of electromigration dispersion and yielded distorted, low R_s values. Therefore, the separations were repeated under the same conditions [2], except that LiOH, which was used to adjust the pH of

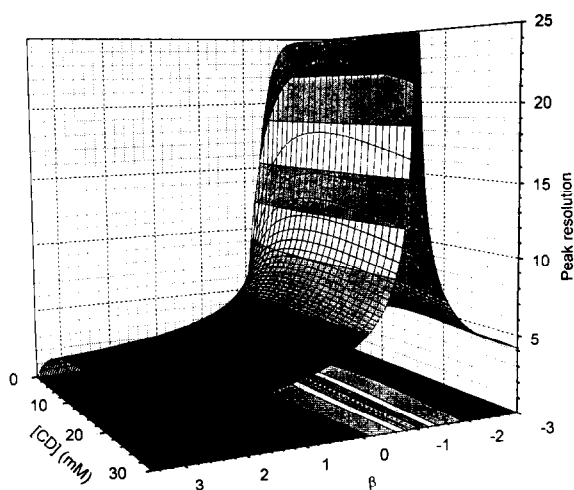


Fig. 6. Peak resolution surface for the enantiomers of homatropine as a function of the cyclodextrin concentration of the background electrolyte and the dimensionless electroosmotic flow coefficient, β , calculated with $E = 600$ V/cm, $l = 39.5$ cm, $T = 310$ K, pH 6.0 and the parameters listed in Table 1.

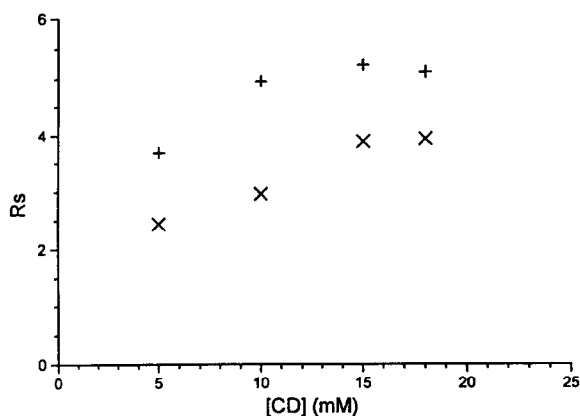


Fig. 7. Comparison of the measured and calculated peak resolutions for the enantiomers of homatropine as a function of the CD concentration at pH 6.30. \times = Measured values; $+$ = calculated values. Conditions: 35 mM H_3PO_4 solution adjusted to pH 6.30 with Jeffamine 900, 0.2% (w/w) 250MHR PA hydroxyethylcellulose (Aqualone), 200 V/cm $< E < 700$ V/cm, $0 < \beta < 0.5$.

the 35 mM phosphoric acid solution to 6.25, was replaced by Jeffamine 900, that has a much lower ionic mobility than Li^+ . The measured and calculated R_s values are shown in Fig. 7 as a function of the cyclodextrin concentration. The trends are identical, except that the measured R_s values are about 20 to 30% lower than the calculated ones indicating that the electromigration dispersion could not be completely eliminated with the Jeffamine 900 base. The electropherogram of homatropine obtained with the [CD] = 18 mM BGE is shown in Fig. 8.

5. Conclusions

The extended peak resolution equation, which contains the effective portion of the applied potential, the temperature, the separation selectivity, the effective charges of the solutes and the dimensionless electroosmotic flow coefficient as variables [3], has been combined with the multiple equilibria-based electrophoretic mobility model [1,2] which describes chiral CE separations as a function of the pH and the β -cyclodextrin concentration of the background electrolyte. Using the mobility model parameters of ibu-

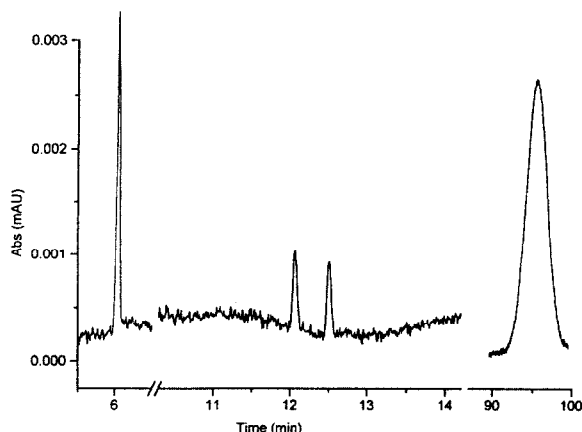


Fig. 8. Electropherogram of a racemic homatropine sample. BGE: [CD] = 18 mM in 35 mM H_3PO_4 solution adjusted to pH 6.30 with Jeffamine 900, 0.2% (w/w) 250 MHR PA hydroxyethylcellulose (Aqualone). $\mu_{eo} = 1.6 \cdot 10^{-5}$ cm²/V s, $E = 430$ V/cm, capillary length to detector: 39.8 cm, total length of capillary: 46.4 cm. First peak = benzyltrimethylammonium chloride; second and third peaks = homatropine enantiomers; last peak = benzylalcohol (electroosmotic flow marker).

profen, a weak acid [1], and homatropine, a weak base [2], the resolution surfaces were calculated for a Type I and a Type III chiral separation. It was found that in Type I separations useful resolution can be obtained only over a narrow pH range (about 2–3 units wide), in the vicinity of the pK_a value. In Type I separations the concentration of cyclodextrin is not as critical a variable as the pH as long as its value is above a minimum level. For Type III separations, the resolution surface has two lobes which are separated by an $R_s(pH, [CD]) = 0$ line. The migration order of the enantiomers changes as one moves from the primary lobe to the secondary lobe, which offers a distinct advantage in trace component analysis.

Peak resolution was found to depend strongly on the value of the dimensionless electroosmotic flow coefficient. Impressive resolution enhancements could be seen in the $-3 < \beta < 1$ range. Using uncoated fused-silica capillaries and hydroxyethylcellulose as electroosmotic flow-suppressing agent, both the $-2 < \beta < -1$ range and

the $-1 < \beta < 0$ range can be utilized to enhance the separation of negatively charged analytes (such as ibuprofen). Without the use of capillaries with a positive surface-charge, only the resolution enhancement that is seen in the $0 < \beta < 1$ range is available experimentally for the positively charged analytes (such as homatropine).

It has been shown that the loci of the pH-induced and CD concentration-induced R_s maxima are not shifted significantly as the β values are changed. This fact allows one to first optimize the selectivity of the separation and then, if needed, independently increase the observed peak resolution by adjusting the value of β .

The utility of the model has been demonstrated by comparing actual measured and calculated R_s values. The $R_s(pH)$ and $R_s([CD])$ trends agreed well, but the measured peak resolutions were consistently lower than the calculated ones indicating that additional peak broadening phenomena, most likely electromigration dispersion, also contributed to the measured widths of the peaks.

Further work is under way in our laboratory to extend the use of the peak resolution and chiral selectivity models to other solute types and other separation-enhancing agents as well.

Acknowledgements

Partial financial support of this project by the National Science Foundation (CHE-8919151), the Advanced Research Program of the Texas Coordinating Board of Higher Education (Grant No. 010366-016), Beckman Instruments Co. (Fullerton, CA, USA), the R.W. Johnson Pharmaceutical Research Institute (Spring House, PA, USA), and the Dow Chemical Co. (Midland, MI, USA) is gratefully acknowledged. The authors are also indebted to American Maize Products Corporation (Hammond, IN, USA) and the Aqualon Corporation (Wilmington, DE, USA), respectively, for the donation of the β -cyclodextrin and the hydroxyethylcellulose samples used in this work.

References

- [1] Y.Y. Rawjee, D.U. Staerk and Gy. Vigh, *J. Chromatogr.*, 635 (1993) 291.
- [2] Y.Y. Rawjee, R.L. Williams and Gy. Vigh, *J. Chromatogr. A*, 652 (1993) 233.
- [3] Y.Y. Rawjee and Gy. Vigh, *Anal. Chem.*, 66 (1994) 619.
- [4] Y.Y. Rawjee, R.L. Williams, L.A. Buckingham and Gy. Vigh, *J. Chromatogr.*, submitted for publication.
- [5] W. Friedl and E. Kenndler, *Anal. Chem.*, 65 (1993) 2003.